Chemistry, Physics and Technology of Surface. 2025. V. 16. N 4. P. 590-602

PACS 82.70.-y, 82.70.Dd, 83.80.Hj, 83.60.Rs, 82.35.Np, 87.85.jf doi: 10.15407/hftp16.04.590

V.A. Prokopenko, A.V. Panko, O.A. Tsyhanovych, I.V. Zatovsky, S.M. Dybkova, L.S. Rieznichenko

ROLE OF COMPONENTS IN AGGREGATE AND STRUCTURE FORMATION IN MULTICOMPONENT "COAGULOX_N" DISPERSIONS

F.D. Ovcharenko Institute of Biocolloidal Chemistry of National Academy of Sciences of Ukraine
42 Academician Vernadsky Blvd., Kyiv, 03142, Ukraine, E-mail: ibcc.ukraine@gmail.com

The diverse applications of dispersed polymineral composites in liquid dispersion media of various types require detailed investigation of the interactions between their components, in order to predict system stability and maintain the necessary physicochemical characteristics. Within the framework of the present study, we analyze the results of the mutual influence of the components of the topical experimental wound-healing, antimicrobial, and hemostatic agent Coagulox_N, which is based on metakaolin, highly dispersed silica (A-300), a plant water-ethanol extract (unripe walnut fruits), and silver and gold nanoparticles. The experimental data obtained are based on measurements of aggregate (particle) size, ζ-potential, rheological, and structural-mechanical characteristics for single- and multiphase aqueous and aqueous-ethanolic systems using a range of modern research methods. The influence of cationic surfactants and several other functional factors on the aggregative stability, structural-mechanical properties, and their controllability in the studied compositions is also considered. It is shown that the aggregation of metallic nanoparticles (silver and gold) occurs already at the stage of their preparation, after which they behave as separate binary phases. The mineral components of the composition form both individual and mixed aggregates of considerable size. In combination, the high values of rheological parameters and their ratios confirm the pronounced thixotropy and plasticity of the developed systems, which meet the requirements for such biomedical materials. Thus, the obtained results make it possible to propose approaches for creating a new stable mineral gel-like medicinal composition with complex action and to outline ways for further improvement of similar systems.

***Keywords**: mineral dispersed materials, colloidal interactions, zeta potential, structure formation, silica, metakaolin, walnut extract, gold and silver nanoparticles, alcoholic extract of unripe walnut, medical composition*

INTRODUCTION

The paper presents the results of research on such systems and the main interactions that occur in them, obtained during the creation of the complex application wound healing, antimicrobial, hemostatic agent "Coagulox_N". This material exerts a combined effect on the hemostatic system, which consists of both direct activation of procoagulant reactions upon contact with blood and indirect stimulation of mechanisms that enhance fibrin formation in the wound. Such an effect is determined by the action of its components: the basis of Coagulox_N is represented by highly dispersed mineral phases of metakaolin and silica, with the dispersion medium being an alcoholic extract of plant raw material – unripe walnut fruits. Metakaolin acts as an activator of the contact phase of hemostasis, triggering prothrombinase formation mechanisms, which result in "cementation" of the primary thrombus; together with silica, it sorbs biologically active toxins in the wound, preventing their interference with normal fibrin formation, and promotes enhanced fibrinolysis at the wound site. The walnut extract serves as an essential component for stopping bleeding and also acts as a preservative [1–4]. Enhancement of the therapeutic properties of the preparation – particularly antimicrobial, wound-healing, anti-edematous, and hemostatic effects, including activity against antibiotic-resistant bacterial strains – along with its consumer characteristics, is achieved by introducing biocompatible spherical silver and gold nanoparticles with an average size of 30 nm, glycerol, and a cationic surfactant into the composition. The high therapeutic efficacy of silver and gold nanoparticles is attributed to their combined effects: antimicrobial activity against a broad spectrum of Gram-positive and Gram-negative microorganisms, including antibiotic-resistant strains; anti-inflammatory and anti-edematous activity (nanoparticles accelerate the transition of

the inflammatory process to the proliferation and organization stages of the affected tissues); and regenerative activity (promoting rapid tissue regeneration, including bone tissue) [5].

MATERIALS AND METHODS

The composition of Coagulox_N consists of (100 %):

- as dispersed phases – metakaolin (heat treated kaolin [1]) (3–7 %), highly dispersed silica A-300 (Kalush, Ukraine) (10–20 %), nanosized silver particles (0.8 mg per 100 g of dispersion), and nanosized gold particles (19.3 μg per 100 g of dispersion) [6];
- as a dispersion medium – water-alcohol (35 % v/v ethanol) extract of unripe walnuts [7], optionally containing glycerol (up to 10 %) and up to 1 % of surfactants and pH regulators (e.g., bis-quaternary ammonium surfactants, sodium citrate, *etc*.).

Silica A-300, metakaolin and their mixture are biocompatible and biosafe mineral compounds for topical use in medicine [8–12]. Water-alcohol extract of unripe walnuts is safe [13] too. Minor additives such as glycerol and other optional regulators are safe ingredients commonly used in medicine.

The size distribution of silver and gold particles in aqueous systems, as well as the relationships between their characteristics and properties, was studied using the dynamic light scattering (DLS) method with a Zetasizer Nano ZS laser correlation spectrometer (Malvern Instruments Ltd., UK) equipped with a helium-neon laser ($\lambda = 632.8$ nm). Also the photon correlation light scattering method (dynamic light scattering, DLS) implemented on a BeNano 90 Zeta spectrometer (Dandong Bettersize Instruments) was used.

The zeta potential (ζ) of the nanoparticles was measured using the same instrument as for DLS by electrophoretic light scattering (sample volume 1 mL, $T = 25$ °C). The ζ-potential was calculated with the standard software package based on Henry’s equation using the Smoluchowski approximation, derived from the electrophoretic mobility of particles in an oscillating electric field at 150 V [14, 15].

SEM imaging was done on a scanning electron microscope Tescan Mira 3 LMU, equipped with energy-dispersive and wavelength-dispersive spectrometers.

Structural-mechanical characteristics of mineral dispersions were determined by the method of tangential displacement of a corrugated plate within the system volume under the application of a constant shear stress, which was gradually increased in each experiment until the system failure. The deformation–time curves $\varepsilon = f(t)$ at different constant shear stresses (P_1, P_2, …, P_n = const) were constructed using a LVDT sensor installed in the Weiler–Rebinder apparatus [16].

The rheological properties of the studied dispersions were determined using a rotational viscometer Rheotest 2 (Medingen GmbH, Germany) with a cylindrical measuring system at shear rates ranging from 0.15 to 1312 s^{-1}. The diameter of the outer cylinder was $R = 20$ mm, with a ratio of outer to inner cylinder radii of $R/r = 1.02$.

The structural (effective) viscosity was calculated as the ratio of shear stress to shear rate ($\eta = P/\gamma$), without correction for the non-Newtonian nature of the flow. Rheological data were automatically transferred to a PC, where further calculations and data processing were carried out. The duration of exposure at different shear rates was 5–30 min.

RESULTS AND DISSCUSSION

Nanosized silver and gold particles in the “Coagulox_N” system. There is a set of criteria and characteristics defined for nanomaterials intended for use in the production of innovative therapeutic agents, in particular the ISO/TS 20660:2019 [17]. This document specifies the physicochemical parameters of AgNP, including average nanoparticle size, zeta potential, nanoparticle concentration, stabilizer, and others. For AuNP, no dedicated document exists, except for the [18]. At the F.D. Ovcharenko Institute of Biocolloidal Chemistry of NAS of Ukraine, nanosized gold and silver particles are synthesized using original protocols based on chemical reduction, including the use of “green” precursors. The biosafety of these nanomaterials is evaluated in accordance with [19], and they are considered promising components for the innovative therapeutic agent Coagulox_N.

The zeta potential (ζ) of the nanoparticles – which, as is well known [14, 15, 20], characterizes their surface properties and temporal stability.

Fig. 1 shows the dependence of the ζ-potential of an aqueous AgNP dispersion (C_{AgNP} = 0.074 mmol/L; the stock solution of 0.8 mg/mL was diluted 100-fold) on the pH of the dispersion medium. As can be seen from Fig. 1, the absolute value of the ζ-potential for the AgNP system increases when moving from acidic to neutral and alkaline conditions.

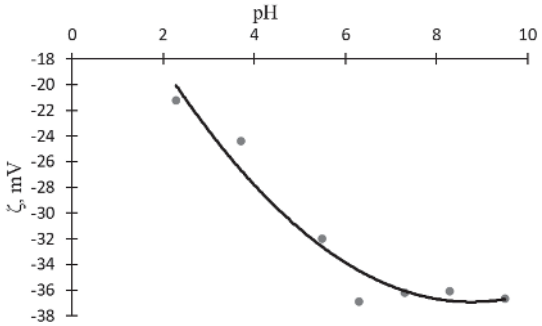

Fig. 1. Dependence of the ζ-potential of an aqueous AgNP dispersion on pH. C_{AgNP} = 0.074 mmol/L

At the same time, the critical ζ-potential value of –30 mV is reached at a pH of about 5, after which it follows a similar trend with increasing pH values toward neutral and alkaline media. The critical value of –30 mV represents the threshold that characterizes the long-term stability of the system: when the ζ-potential is ≥ |30| mV, the nanostructures are considered stable and resistant to aggregation [14, 20].

This can be explained by the fact that at pH ≤ 5, the surface atoms of silver participate in the formation of an oxide film of Ag_xO (up to Ag_2O under strongly acidic conditions [21, 22]). Under certain spatial and hydrodynamic conditions, this leads to the formation of chemical bonds between the particles and, consequently, to their aggregation.

At pH ≥ 5, these processes are suppressed: the oxidation of surface silver atoms by dissolved oxygen is replaced by the presence of a sufficient amount of competing OH^- ions in the dispersion medium. This results in the "forced" hydration of the silver particle surfaces, which should be reflected in an increase (in absolute values) of the ζ-potential and in the overall aggregative stability of the system. This is indeed observed in the dependence shown in Fig. 1, which illustrates the proposed mechanism: the ζ-potential increases up to –37.2 mV, and the subsequent Fig. 2 demonstrates the corresponding change in the particle size distribution of the system as it shifts from acidic pH values to those close to neutral.

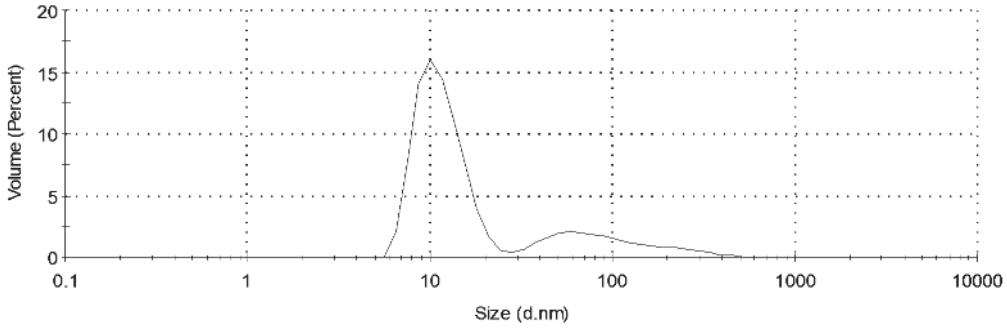

Fig. 2. Size distribution of nanoparticles in aqueous AgNP dispersion (C_{AgNP} = 0.074 mmol/dm³) at pH 5.5

As shown in Fig. 2, at pH 5.5 the aqueous AgNP dispersion is dominated by particles with a size of 11.6 nm (79 %), while a smaller proportion of particles with a size of 80 nm (21 %) is also present.

At identical conditions at pH 2.3, our experimental results indicate that the system is dominated by particles of 101.9 nm (88 %), with an additional fraction of 5.2 μm particles (12 %).

This observation correlates well with the ζ-potential dependence of the system on pH.

Replacement of the aqueous dispersion medium with a water-ethanol unripe walnut extract led to enhanced aggregation processes compared to the purely aqueous system. Under the same conditions, silver particles with sizes of 17.5, 75, and 135 nm were identified. The relative volume ratio of particles (estimated from the area under the peaks) in the 17.5 nm region to those in the 75–135 nm region was approximately 40:50, indicating that the system is dominated by larger, aggregated particles.

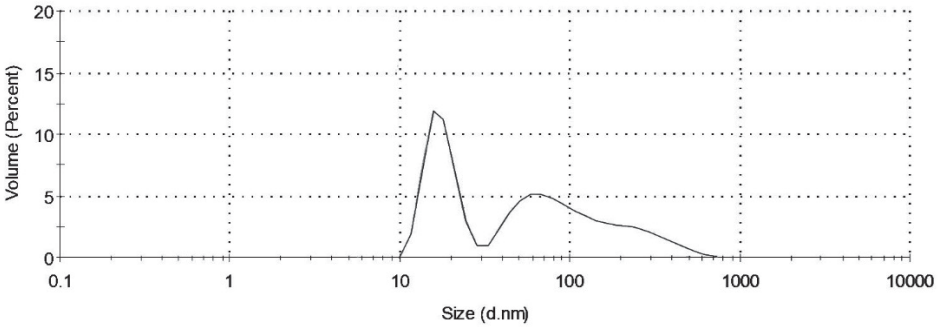

Fig. 3. Size distribution of nanoparticles in AgNP dispersion based on alcoholic extract of unripe walnut fruits at pH 5.5

The study of gold-containing systems (AuNP) (Fig. 4) demonstrated that, in the acidic pH range, they are not stable against aggregation, similar to the silver-containing systems described above. Increasing the pH to 7 results in relatively high ζ-potential values (–37 mV) for the gold aqueous sol, with 99 % of the particles having a size of about 4.5 nm (Fig. 5 *a*). This indicates a high stability of the system in neutral and alkaline media.

Gold particles in studied plant extract (Fig. 5 *b*) are predominantly observed at a size of about 7 nm, which is nearly 40 % larger than the particle size in the aqueous medium. In addition, this system contains more than 2 % of aggregates with a size of 4.6 μm. The ζ-potential of this system is below –30 mV, which, by analogy with silver-based systems, is lower than the stability threshold for nanosized gold particles. Thus, even in the case of gold nanoparticles, replacing the aqueous medium with a water-ethanol unripe walnut extract induces aggregation processes.

For the development of a multiphase complex therapeutic agent such as *Coagulox_N*, the use of nanosized particles of both silver and gold is required, which raises the question of their interactions upon introduction into a water-ethanol dispersion medium.

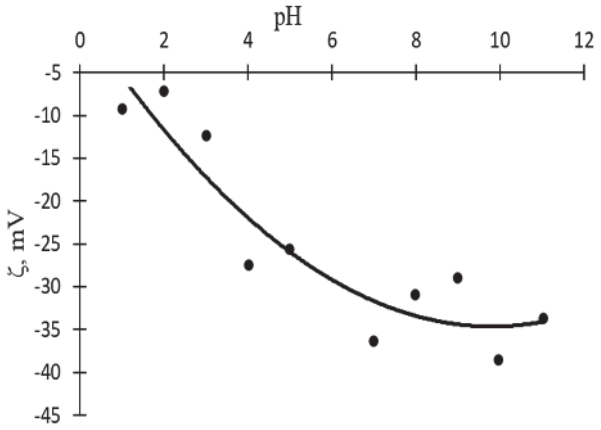

Fig. 4. Dependence of the ζ-potential of an aqueous AuNP dispersion on pH. C_{AuNP} = 0.01 mmol/dm³

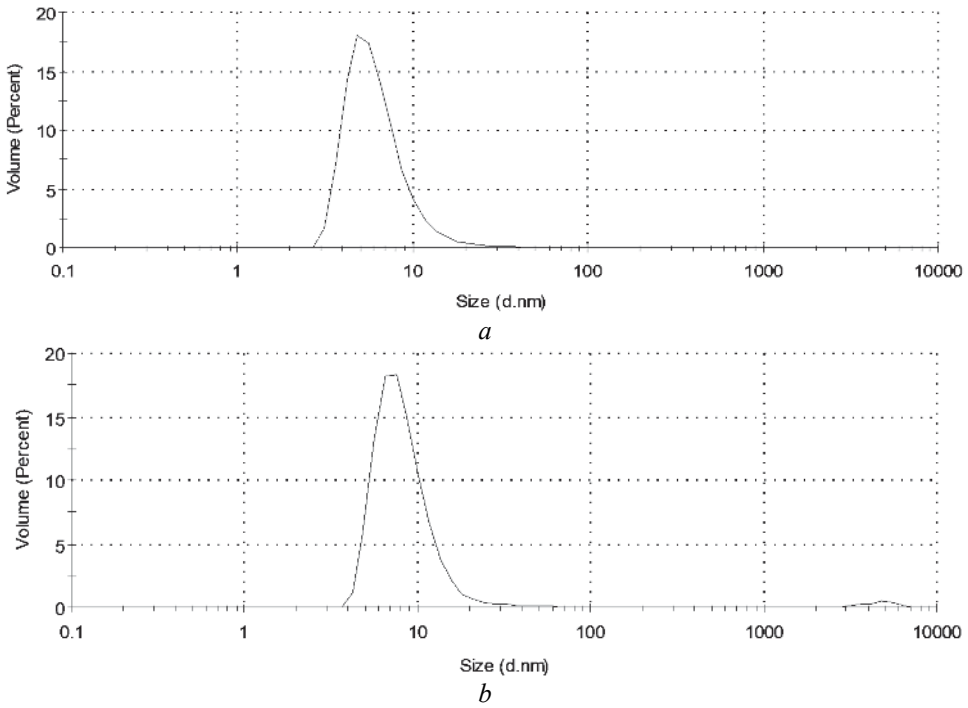

Fig. 5. Size distribution of gold particles in aqueous dispersion (*a*) and in AuNP dispersion with studied plant extract (*b*) at pH 7.3

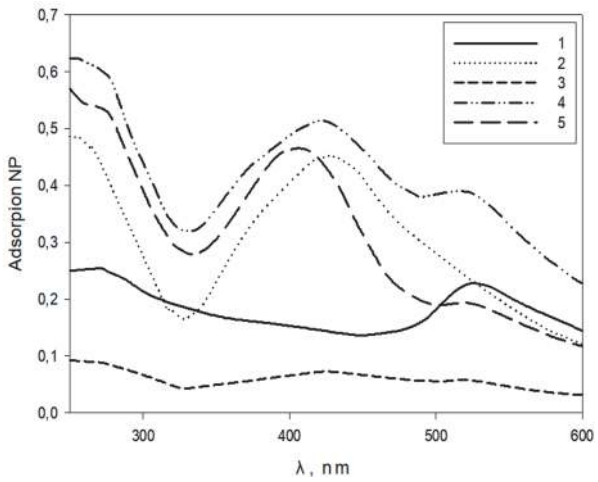

Fig. 6. UV–vis absorption spectra of nanoscale systems: *1* – AuNP, *2* – AgNP, *3* – unripe walnut extract, *4* – AgAuNP (1.25:0.1 aqueous dispersion), *5* – AgAuNP (1.25:0.1 in studied plant extract)

Spectrophotometric studies of dispersions containing silver and gold nanoparticles are illustrated in Fig. 6. Differences in the absorption bands indicate the formation of nanoscale systems and the coexistence of AgNP and AuNP in both the aqueous dispersion and the walnut fruit extract; no other compounds were detected. The absorption maximum of the aqueous AgNP dispersion at 424 nm corresponds to particles 20–50 nm in size, while λ_{max} for AuNP at 528 nm corresponds to particles 15–40 nm [23, 24]. In the absorption bands of the AgAuNP systems (curves 4 and 5), two distinct maxima are observed, which correspond to silver and gold particles (aggregates). This finding correlates with the particle size distribution obtained by DLS and with the data from SEM images of silver and gold particles in aqueous medium (Fig. 7).

This image demonstrates that heterogeneous but similarly sized silver and gold nanoparticles in aqueous medium form composite AgNP and AuNP aggregates, despite having the same

surface charge sign, as characterized by the ζ-potential, and the similarity of their relatively high values (–36.5 mV for AgNP and –35.0 mV for AuNP).

Fig. 8 presents SEM images of silver and gold particles in a water–ethanol walnut extract, which, similar to the case of the water–ethanol dispersion medium, also reveals aggregates of heterogeneous particles across a wide size range.

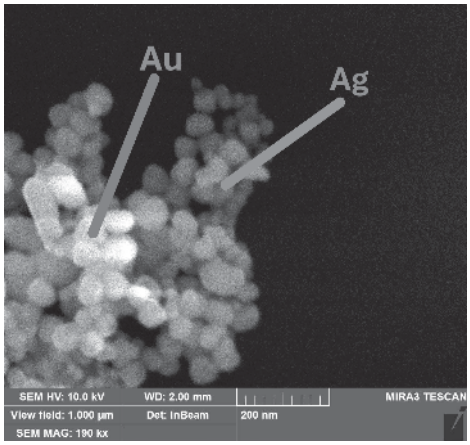

Fig. 7. SEM images of silver and gold particles in aqueous medium

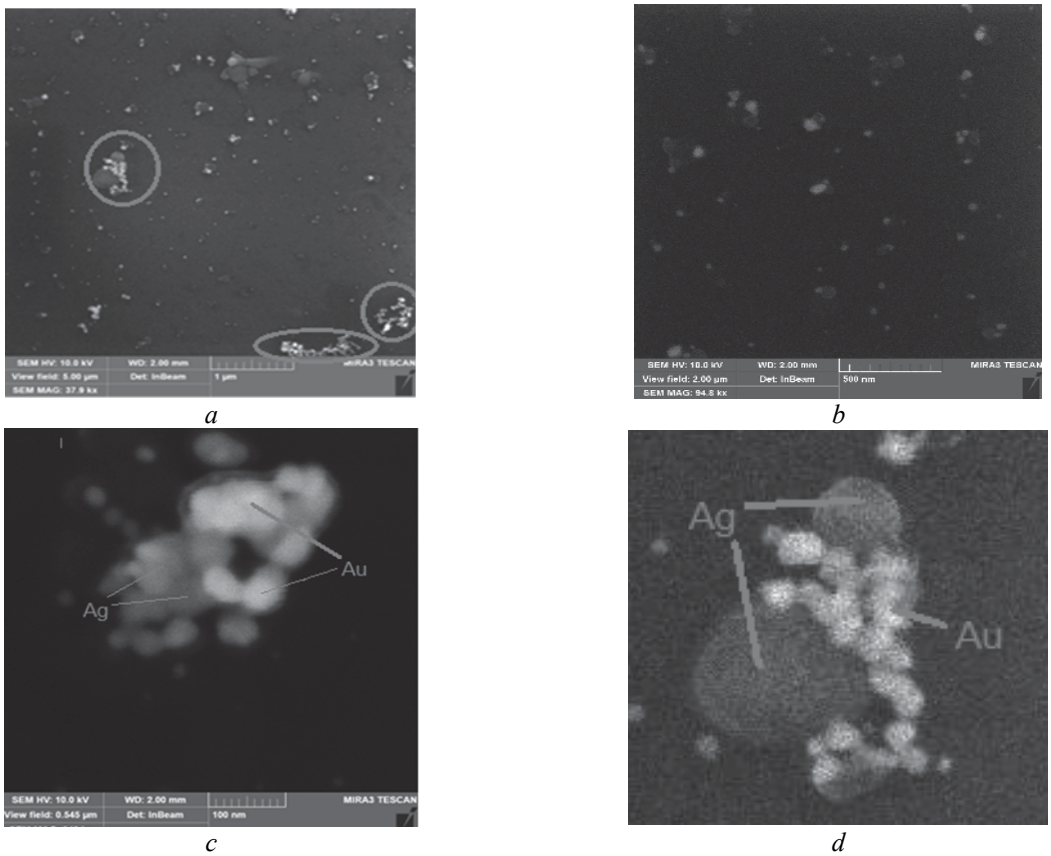

Fig. 8. SEM images of silver and gold particles in a water–ethanol walnut extract: (*a*) general view of silver and gold particles (aggregates) within a 5×5 µm area; (*b*) same within a 2×2 µm area; (*c*) view of a representative average-sized particle (aggregate) within a 0.543×0.543 µm area; (*d*) fragment of the image shown in Fig. 8 *a*

The images in Fig. 8 show that the primary particle size of silver is about 20–50 nm, while that of gold is 15–40 nm, in agreement with the spectrophotometry results and, overall, the DLS data. At the same time, the images (Fig. 8 *c*, *d*) clearly illustrate the aggregative nature of the systems, where the dispersed phase consists of aggregates formed from primary silver nanoparticles onto which primary gold nanoparticles are deposited.

The majority of such aggregates are up to 100 nm in size (Fig. 8 *a*–*c*), although a certain number of larger aggregates exceeding 200 nm are also present (circled in Fig. 8 *a*, and visible in Fig. 8 *d*).

Aggregation in the multicomponent system "Coagulox_N". Using the photon correlation light scattering method (dynamic light scattering, DLS), the size distribution of nano- and ultradispersed particles (aggregates) of the multicomponent system modeling *Coagulox_N* was determined. As noted above, the system includes highly dispersed silica A-300, metakaolin, and nanosized metals in aqueous and aqueous–alcoholic dispersion media, diluted 1000-fold with distilled water (*a*) or with an aqueous–alcoholic solution (*b*) of the same concentration as that used for preparing this model system without walnut extract and modifier additives (Fig. 9).

The addition of glycerol to the studied model system in the amount specified above (10 %), followed by 1000-fold dilution with the aqueous–ethanolic solution, reduces the particle (aggregate) size to 152 nm, while the ζ-potential increases significantly to +15 mV at pH 5.5 (Fig. 10 *a*).

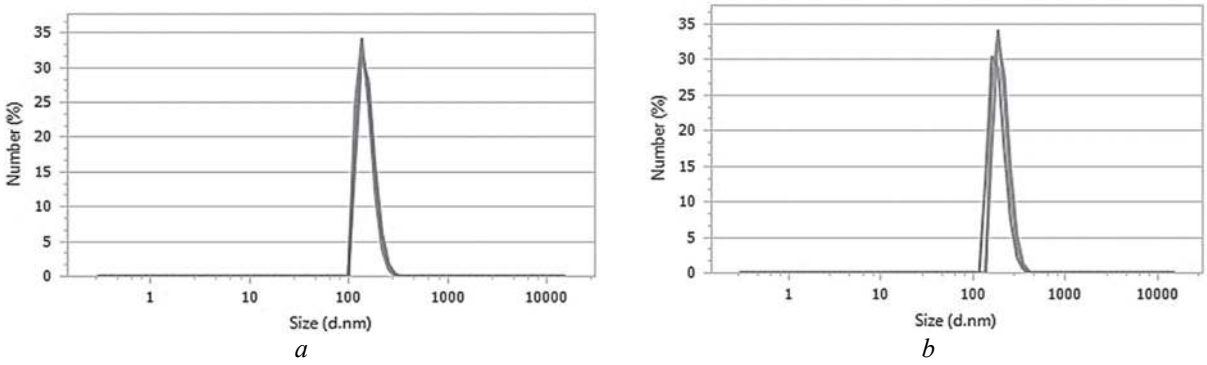

Fig. 9. Size distribution of particles (aggregates) of the model material in aqueous (*a*) and aqueous–ethanolic dispersion media (*b*)

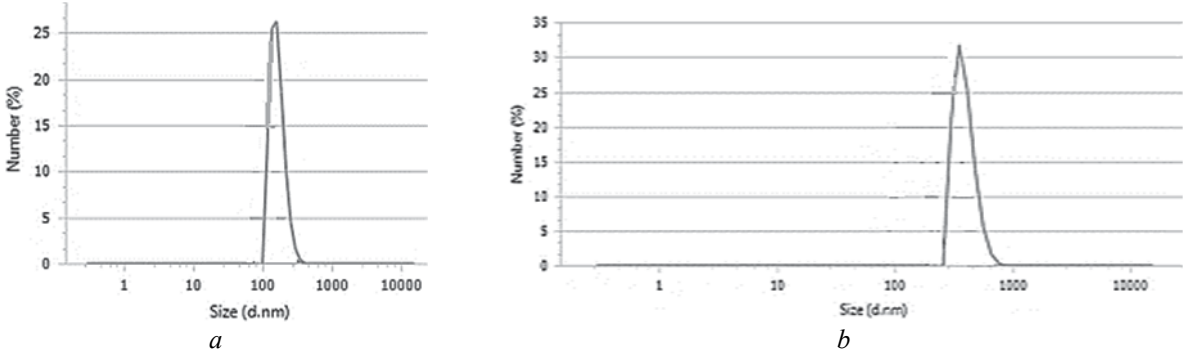

Fig. 10. Size distribution of particles (aggregates) of the model material in aqueous–ethanolic dispersion medium in the presence of glycerol (*a*) and glycerol with a cationic surfactant (*b*)

In the presence of a cationic surfactant (0.5% in the initial composition) (Fig. 10 *b*), the average particle (aggregate) size increases more than twofold, reaching 348 nm, while the ζ-potential rises to +37.3 mV (pH 4.1).

Replacing the water–ethanol dispersion medium (Fig. 10) with a water–ethanol extract (Fig. 11) does not cause significant changes in the system compared to the model system containing glycerol and a cationic surfactant. This is

confirmed by Fig. 11, which shows an average particle (aggregate) size of 298 nm, a ζ-potential of 31.7 mV, and a pH of 4.4.

The appearance of system fragments, particularly as shown in the SEM images (Fig. 12 *a*, *b*), indicates that virtually all particles are present in aggregates, which are distributed across a wide size range.

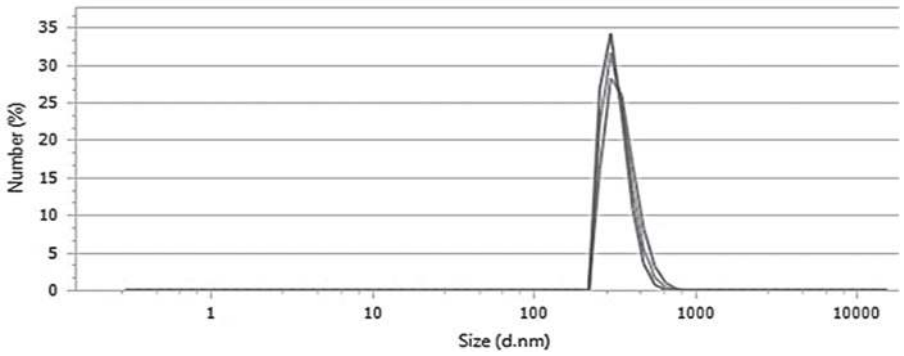

Fig. 11. Size distribution of particles (aggregates) of C*oagulox_N* in a water–ethanol extract with 10 % glycerol and 0.5 % cationic surfactant

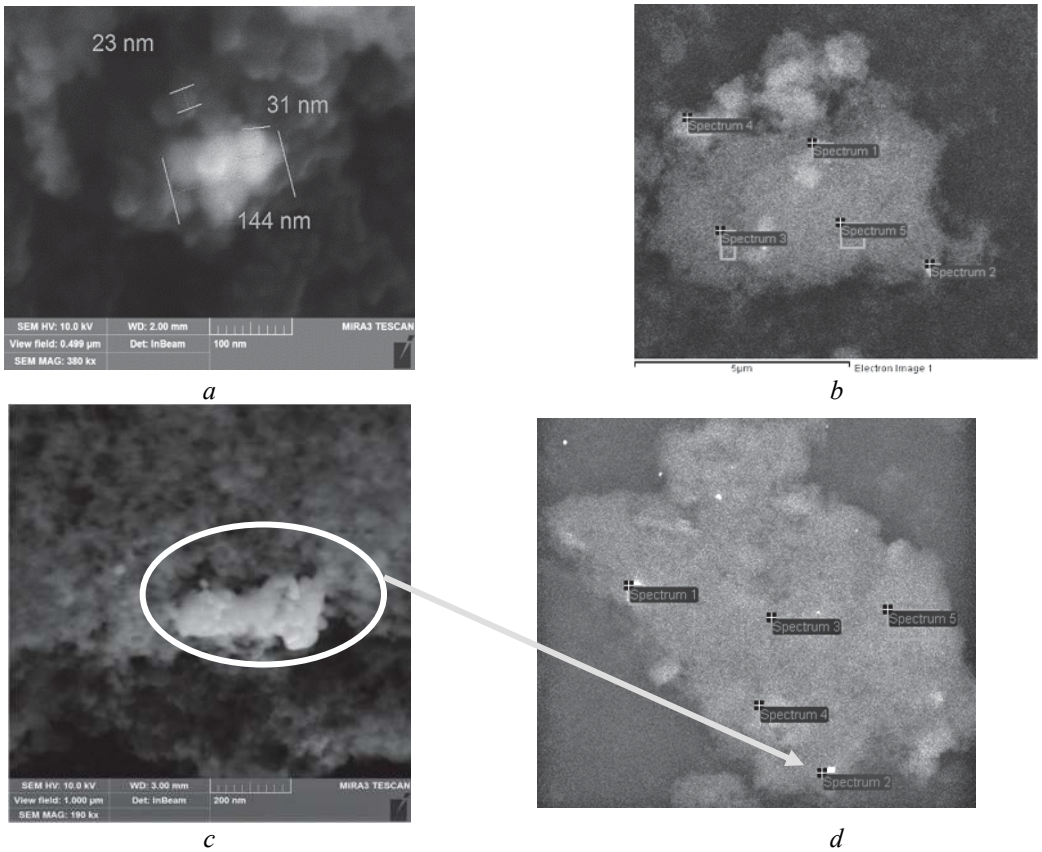

a *b*

c *d*

Fig. 12. SEM images of aggregates–the structural components of the therapeutic material *Coagulox_N* in a water–ethanol extract: (*a*) with annotated particle sizes; (*b*, *d*) with locations for spectral elemental composition analysis; *c* – enlarged image of an aggregate of silver particles located on a larger “Coagulox_N” aggregate (*d*)

The elemental composition of randomly selected aggregates, presented in Tables 1 and 2 and illustrated by the spectra in Figs. 13 and 14, indicates that the aggregates are formed from particles of different nature – representing all phases present in the *Coagulox_N* material:

highly dispersed silica, metakaolin, silver, and gold.

Analysis of the presented data suggests that the studied material is a dispersed system consisting of structured aggregates – composites in which nanosized particles of highly dispersed silica, up to 5–10 μm in size (spectra 1 and 5 in Fig. 12 *b*, *d*), are combined with metakaolin particles of up to 1 μm (spectrum 4 in Fig. 12 *b*, *d*). Silver–gold aggregates, and occasionally silver alone (due to the considerably higher silver concentration compared to gold), are located on the surface of silica aggregates or on the surface of metakaolin particles (aggregates).

Table 1. Elemental composition of the aggregate (Fig. 12 *b*) of the *Coagulox_N* sample in a water-ethanol extract in the presence of glycerol and a cationic surfactant

Spectrum	C	O	Al	Si	K	Ag	Au	Total
Spectrum 1	20.82	36.03	1.48	17.74		20.69	3.24	100.00
Spectrum 2	59.67	21.82	0.15	7.16		11.21		100.00
Spectrum 3	55.47	27.86	0.20	11.55		4.91		100.00
Spectrum 4	45.40	34.39	7.42	11.86	0.93			100.00
Spectrum 5	50.44	34.15	0.31	15.09				100.00

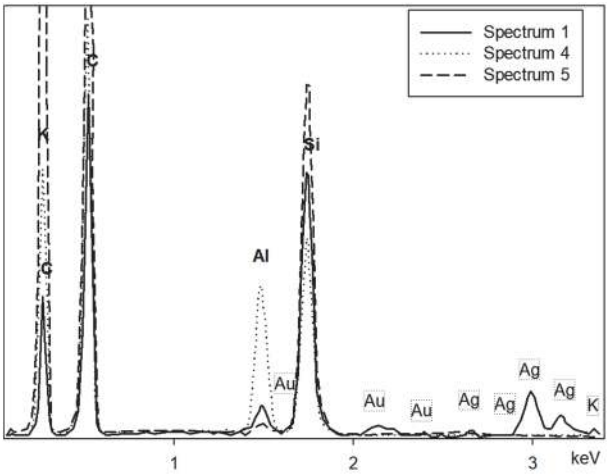

Fig. 13. X-ray fluorescence spectrum of the elemental composition of particles forming the aggregates of Coagulox_N (Table 1)

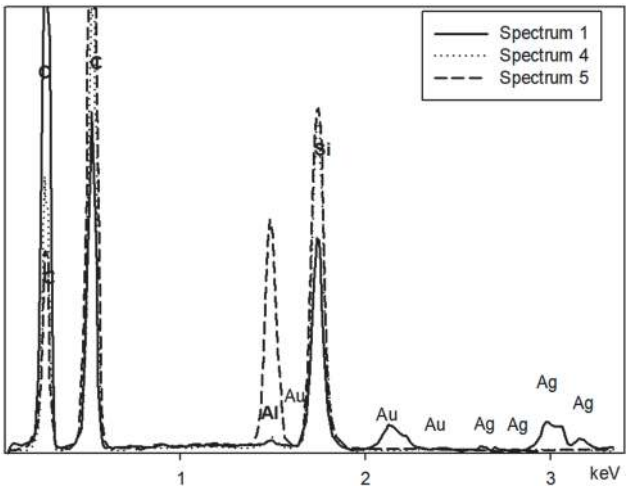

Fig. 14. X-ray fluorescence spectrum of the elemental composition of particles forming the aggregates of *Coagulox_N* (Table 2)

Table 2. Elemental composition of an aggregate (Fig. 12 *d*) of the Coagulox_N sample in a water–ethanol extract in the presence of glycerol and a cationic surfactant

Spectrum	C	O	Al	Si	Ag	Au
Spectrum 1	67.34	25.25	0.12	5.30	1.43	0.57
Spectrum 2	75.94	19.66	0.16	3.46	0.78	
Spectrum 3	38.83	44.12	0.71	15.31	1.03	
Spectrum 4	38.45	45.19	5.97	10.39		
Spectrum 5	52.07	36.30	0.36	11.27		

Structural-mechanical and rheological properties of the studied composition. The regularities described above were obtained in studies of diluted dispersed systems. However, when the formation of such composite aggregates occurs under conditions of high mass concentration, and therefore high particle concentration (approximately 15–20 wt.% of the mineral solid phase), interparticle interactions lead to the aggregation of particles of different nature. As a result, a coagulation structure [25] is formed throughout the entire volume of the dispersion, which ensures its high kinetic stability and thixotropic properties.

To describe the deformation processes in such systems under the action of constant shear stress, the generalized Maxwell–Shvedov–Kelvin model [16, 26] was used. According to this model (at P = const), the shear strain ($\acute{\varepsilon} = \varepsilon/a$) is determined by the equation:

$$\varepsilon' = \frac{P}{G_1} + \frac{(P - P_{K1}) \cdot t}{\eta_1} + P\frac{1 - \exp\left(-t\frac{G_2}{\eta_2}\right)}{G_2},$$

where P and P_{K1} are the shear stress and the conditional static yield stress, respectively; η_1 and η_2 are the maximum plastic viscosity and the viscosity of slow elastic deformation; G_1 and G_2 are the shear moduli of fast and slow elastic deformations, respectively.

Based on the components of this model obtained experimentally – the shear moduli of fast and slow elastic deformations (G_1, G_2), the conditional static yield stress (P_{K1}), and the maximum viscosity of the practically undisturbed structure (η_1) – the following values were calculated according to [26]:

- equilibrium shear modulus $G = \frac{G_1 G_2}{G_1 + G_2}$;
- elasticity $\lambda = \frac{G_1}{G_1 + G_2}$;
- true relaxation time $\theta = \frac{\eta_1}{G}$;
- plasticity $Pl = P_{K1}/\eta_1$,

which, together with the experimentally obtained parameters, provide a quite complete characterization of the studied systems (Table 3).

The data in Table 3 indicate a significant contribution of plasticity and elasticity to the deformation properties of the studied systems [26].

The shear moduli and viscosity of the system increase sharply when the alcoholic solution is replaced with a walnut extract, which promotes interparticle interactions and enhanced structural formation of the system. At the same time, the addition of glycerol and a cationic surfactant reduces all of these parameters, but their values, as demonstrated by in-use tests, ensure the required consumer properties. In particular, the material is able to adhere to surfaces in sufficiently thick layers, does not flow under its own weight, and shows a high capacity to fill surface defects and adhere effectively.

An important aspect of both the application and preparation of topical therapeutic materials based on dispersed systems lies not only in their structural-mechanical, but also in their rheological properties.

Fig. 15 presents the rheogram of *Coagulox_N*, which shows that the system belongs to weak solid-like structures [25], with a significant range of viscosities of the conditionally undisturbed structure η_0 = 64 Pa·s and the maximally disrupted structure η_m = 0.1 Pa·s, respectively. Thus, the system is typically thixotropic, with signs of a viscosity ultraanomaly characteristic for ultradispersed systems [27].

Due to the high tendency of the studied systems to interparticle aggregation, once a certain solid-phase concentration is reached, structure formation occurs throughout the entire

dispersion volume, ensuring its kinetic stability. As found, both the model system "highly dispersed silica – metakaolin – water-ethanol dispersion medium" and the *Coagulox_N* material, at solid-phase concentrations above 13 wt. % in either the water-ethanol medium or the walnut extract, remain kinetically stable due to the structures formed, and are resistant to phase separation over extended periods (more than one year).

Table 3. Structural-mechanical properties of the dispersions "highly dispersed silica – metakaolin – water-ethanol dispersion medium," "highly dispersed silica – metakaolin – walnut extract," and the *Coagulox_N* material

Sample	G_1, kPa	G_2, kPa	G, kPa	P_{K1}, Pa	$\eta_1 \cdot 10^{-5}$, Pa·s	λ	Plasticity $P_{K1}/\eta_1 \cdot 10^6$, s^{-1}	Θ, s
Mixture of silica and metakaolin (10:3) in 35 vol% ethanol	1.8	1.0	0.6	0.1	3.6	0.643	0.278	60
Coagulox_N	47.3	21.8	14.4	48.0	37.2	0.685	12.903	26
Coagulox_N with additives	36.2	17.3	11.3	37.0	12.7	0.677	2.913	11

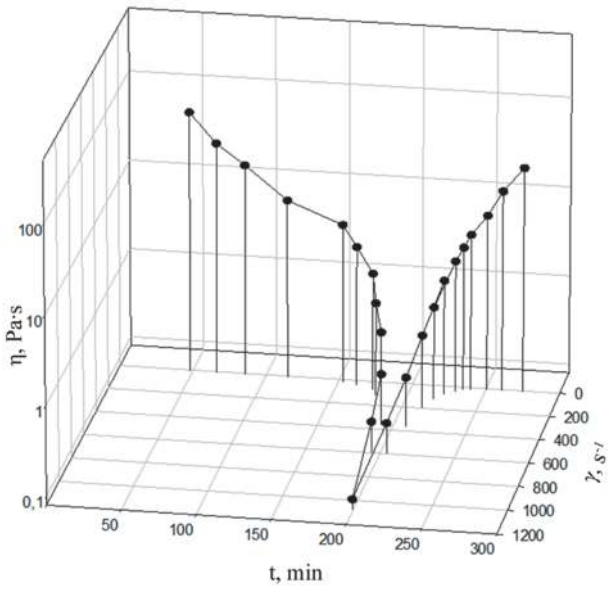

Fig. 15. Rheogram of the wound-healing and hemostatic therapeutic composition *Coagulox_N* (25 °C)

CONCLUSIONS

From the presented experimental results, the following conclusions can be drawn, which should be taken into account in the development of composite materials, particularly for medical applications, based on mineral components.

Already at the stage of obtaining aqueous-ethanolic dispersions of silver and gold nanoparticles, aggregation occurs. Subsequently, during the formation of dispersed systems with mineral ingredients – highly dispersed silica and metakaolin – the aggregates of primary nanosized silver and gold particles behave as separate binary phases.

The mentioned mineral phases that are part of the composite therapeutic material, in turn, demonstrate mutual aggregation ability and form large aggregates both from particles of the same nature and from particles of different mineral phases.

Considering that, in the theory of dispersion stability, the electrokinetic component as a thermodynamic factor (electrostatic repulsion of like-charged particles of the dispersed phase) is often not decisive compared to other thermodynamic and kinetic factors – such as the presence of hydration and adsorption layers on the particle surface, disjoining pressure, *etc*., which in one way or another modify (control) interparticle

interactions – it can be concluded that the ζ-potential has only a minor influence on aggregation processes in the studied systems.

The high values of moduli and rheological parameters characterizing the structural-mechanical and rheological properties of the studied dispersions and composites, as well as their ratios, indicate strong thixotropy and plasticity of the systems. These properties are among the key requirements in the development of materials of this type.

ACKNOWLEDGEMENT

This work was carried out with the financial support of the National Research Foundation of Ukraine (Project No. 2023.04/0041 *“Development of an innovative medicinal product "Coagulox_N" with antimicrobial, hemostatic, and wound healing properties”*).

Роль складових у агрегато- та структуроутворенні в багатокомпонентних дисперсіях «Коагулокс_N»

В.А. Прокопенко, А.В. Панько, О.А. Циганович, І.В. Затовський, С.М. Дибкова, Л.С. Рєзніченко

Інститут біоколоїдної хімії ім. Ф.Д. Овчаренка Національної академії наук України
бульв. Академіка Вернадського, 42, Київ, 03142, Україна, ibcc.ukraine@gmail.com

Різноманітне використання дисперсних полімінеральних композитів в рідких дисперсійних середовищах різної природи вимагають детальних досліджень особливостей взаємодії їхніх компонентів з метою передбачення стабільності та збереження необхідних фізико-хімічних характеристик для такої системи. В рамках представленого дослідження аналізується взаємовплив компонентів аплікаційної форми експериментального ранозагоювального, антимікробного та кровоспинного засобу «Коагулокс_N» на основі метакаоліну, високодисперсного кремнезему (А-300), рослинного водно-спиртового екстракту (незрілі плоди горіху волоського) та наночастинок срібла та золота. Одержані експериментальні дані базуються на основі вимірювань розміру агрегатів (частинок), їхнього ζ-потенціалу, реологічних та структурно-механічних характеристик для одно- та багатофазних водних та водо-етанольних систем з використанням низки сучасних методів досліджень. Також розглянуто вплив катіоноактивних ПАР та ряду інших функціональних факторів на агрегативну стійкість, структурно-механічні властивості та можливості керування ними у розглянутих композиціях. Показано, що агрегація наночастинок металів (срібло та золото) відбувається вже на стадії їхнього одержання, що в подальшому поводять себе як окремі бінарні фази. Мінеральні компоненти композиції формують як індивідуальні, так і змішані агрегати зі значними розмірами. У комбінації виявлені високі значення реологічних показників та їхніх співвідношень засвідчують значну тиксотропію і пластичність розроблених систем, які відповідають вимогам для подібних матеріалів медичного призначення. Відповідно, отримані результати дозволили запропонувати підходи до створення нової стійкої мінеральної гелеподібної медичної композиції комплексної дії та вказати на шляхи подальшого вдосконалення подібних систем та засобів.

***Ключові слова**: мінеральні дисперсні матеріали, колоїдні взаємодії, дзета-потенціал, структуроутворення, аеросил, метакаолін, наночастинки золота і срібла, спиртовий екстракт незрілих плодів горіху волоського, медична композиція*

REFERENCES

1. Patent UA 76662. Pakhovchyshyn S.V., Sukhovii M.V., Petrenko O.O., Panko A.V., Averianov E.V., Semeniaka V.I., Petrenko O.F., Tarnavsky D.V., Smurna O.V., Chukhno V.S., Prokopenko V.A. Wound-healing composition for treating hemophilic patients. 2006. [in Ukrainian].
2. Pakhovchyshyn S.V., Prokopenko V.A., Hryshchenko V.H., Hrytsenko V.F., Sukhovii M.V., Averianov E.V., Mironiuk O.V., Sydorovsky O.Yu. Colloidal-chemical and therapeutic properties of nanoscale systems of clay minerals. *Nanosystems, Nanomaterials, Nanotechnologies*. 2004. **2**(3): 1069. [in Ukrainian].

3. Panth N., Paudel K.R., Karki R. Phytochemical profile and biological activity of Juglans regia. *J. Integr. Med.* 2016. **14**(5): 359.
4. Delaviz H., Mohammadi J., Ghalamfarsa G., Mohammadi B., Farhadi N. A review study on phytochemistry and pharmacology applications of Juglans regia plant. *Pharmacogn. Rev.* 2017. **11**(22): 145.
5. Reznychenko L.S., Rybachuk A.V., Dybkova S.N., Gruzina T.G., Malanchuk V.A., Ulberg Z.R. Nanoparticles of silver and their combination with gold nanoparticles as effective antimicrobial agents for the treatment of purulent-inflammatory diseases in dentistry and maxillofacial surgery. In: *Fundamental problems of creation of new substances and materials of chemical production*. (Kyiv: Akademperiodyka, 2016). [in Ukrainian].
6. Guidelines "Safety assessment of medical nanopreparations" (approved by the Scientific Expert Council of the State Expert Centre of the Ministry of Health of Ukraine, protocol N 8, 09.26.2013), (Kyiv, 2013). [in Ukrainian].
7. TU U 20.4-05402714-007:2025. Prophylactic and hygienic means – liquid alcoholic extracts of walnut. Kyiv, 2025. [in Ukrainian].
8. Zatovsky I.V., Dybkova S.M., Tsyganovich O.A., Dmytrukha N.M., Gruzina T.G., Rieznichenko L.S., Panko A.V., Prokopenko V.A. Biosafety assessment of the experimental innovative medicinal product "Coagulox_N". *Bulletin of problems biology and medicine*. 2025. **178**(3): 113.
9. TECHNICAL INFORMATION TI 1415. AEROSIL® and AEROPERL®. Pharma Colloidal Silicon Dioxide Products - https://products.evonik.com/assets/50/06/TI_1415_EN_EN_245006.pdf
10. Zhang Y., Chen X., Zhao B., Wu H., Yuan L., Zhang H., Dai W., He B., Xing G., Zhang Q., Wang X. Biosafety study and mechanism comparison on two types of silica with different nanostructures. *Toxicol. Res*. 2017. **6**(4): 487.
11. Niculescu A.G., Grumezescu A.M. An Up-to-Date Review of Biomaterials Application in Wound Management. *Polymers*. 2022. **14**(3): 421.
12. Twinprai N., Sutthi R., Ngaonee P., Chaikool P., Sookto T., Twinprai P., Mutoh Y., Chindaprasirt P., Laonapakul T. Effects of hydroxyapatite content on cytotoxicity, bioactivity and strength of metakaolin/hydroxyapatite composites. *Arabian J. Chem*. 2024. **17**(9): 105878.
13. Mukarram S.A., Wandhekar S.S., Ahmed A.E.M., Várallyay S., Pandey V.K., József P., Bela K. Global Perspectives on the Medicinal Implications of Green Walnut and Its Benefits: A Comprehensive Review. *Horticulturae.* 2024. **10**(5): 433.
14. Dukhin S.S. Electrical conductivity and electrokinetic properties of disperse systems. Acad. Sci. UkrSSR. (Kyiv: Naukova Dumka, 1975). [in Russian].
15. Serrano-Lotina A., Portela R., Baeza P., Alcolea-Rodriguez V., Villarroel M., Ávila P. Zeta potential as a tool for functional materials development. *Catal. Today*. 2023. **423**: 113862.
16. Kruglitsky N.N. *Physicochemical bases of regulation of properties of clay mineral dispersions*. (Kyiv: Naukova Dumka, 1968). [in Russian].
17. ISO/TS 20660:2019 (2022 renow). Nanotechnologies – Antibacterial silver nanoparticles – Specification of characteristics and measurement methods. – Geneva: ISO, 2019.
18. ISO/TS 14101:2012 (2023 renow). Surface characterization of gold nanoparticles for nanomaterial specific toxicity screening: FT-IR method. – Geneva: ISO, 2012.
19. Methodical recommendations. Evaluation of the safety of medicinal nanodrugs. (Kyiv, 2013). [in Ukrainian].
20. Clogston J.D., Patri A.K. Zeta potential measurement. *Methods Mol. Biol.* 2011. **697**: 63.
21. Lundahl P., Stokes R., Smith E., Martin R., Graham D. Synthesis and characterization of monodispersed silver nanoparticles with controlled size ranges. *Micro Nano Lett.* 2008. **3**(2): 62.
22. Mock J.J., Barbic M., Smith D.R., Schultz D.A., Schultz S. Shape effects in plasmon resonance of individual colloidal silver nanoparticles. *J. Chem. Phys.* 2002. **116**(15): 6755.
23. Dhara S., Lu C.-Y., Magudapathy P., Huang Y.-F., Tu W.-S., Chen K.-H. Surface plasmon polariton assisted optical switching in noble bimetallic nanoparticle system. *Appl. Phys. Lett.* 2015. **106**(2): 023101.
24. Vinod M., Gopchandran K.G. Au, Ag and Au:Ag colloidal nanoparticles synthesized by pulsed laser ablation as SERS substrates. *Prog. Nat. Sci.: Mater. Int.* 2014. **24**(6): 569.
25. Ovchinnikov P.F., Kruglitsky N.N., Mikhailov N.V. *Rheology of thixotropic systems*. (Kyiv: Naukova Dumka, 1972). [in Russian].
26. Grankovsky I.G. *Structure formation in mineral binder systems*. (Kyiv: Naukova Dumka, 1984). [in Russian].
27. Kovzun I.G., Prokopenko V.A., Panko A.V., Tsyganovich O.A., Oliinyk V.O., Nikipelova O.M., Ulberg Z.R. *Nanochemical, nanostructural and biocolloidal aspects of transformations in dispersions of iron-aluminosilicate minerals*. (Kyiv: Akademperiodyka, 2020).

Received 29.09.2025, accepted 04.12.2025